

Measurements and 3D simulation of novel ATLAS planar pixel detector structures including edgeless and alternative bias grid geometries for the HL-LHC upgrade

PIXEL 2014, Niagara Falls, Canada

N. Dinu, E. Gkougkousis, A. Lounis, C. Nellist

Laboratoire de l'Accélérateur Linéaire

2nd September, 2014



Introduction

Motivation

Laboratory Characterisation

Test structures

Characterisation

Source scans

SIMS

Preparation of samples

Simulation

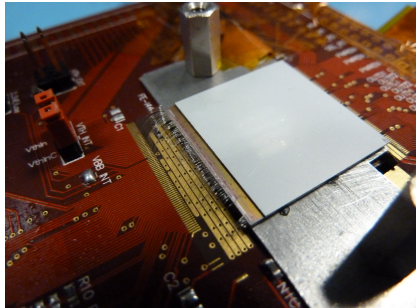
Results

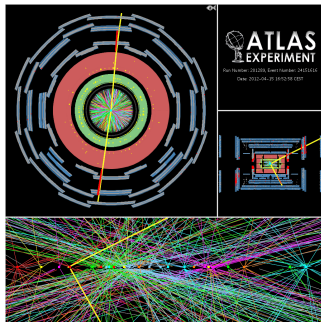
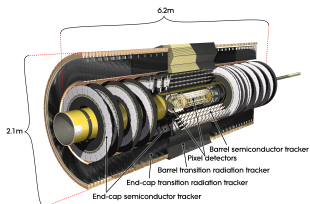
Future Plans

Irradiation plans

Further plans

Summary





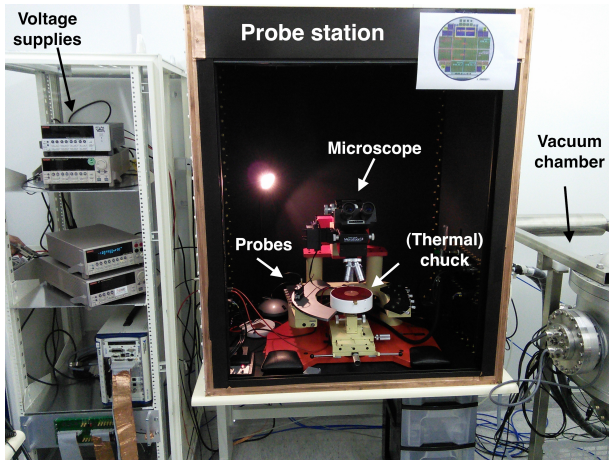
- HL-LHC phase II upgrade in ~ 2022
- All silicon tracker with greater area of pixel detectors
 - Expected fluence of $\sim 2 \times 10^{-16}$ in the innermost layer ($\sim 4\text{mm}$)
- Includes a new ATLAS pixel layer \rightarrow requires improved pixel devices
 - radiation hard
 - slimmer edges
 - better granularity... etc

Planar Pixel Sensors

Part of the ATLAS ITk Sensor Group.

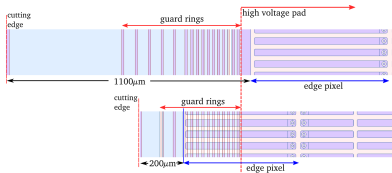
- Switzerland
 - CERN
 - University of Geneva
- Czech Rep
 - AS CR, Prague
- France
 - LAL Orsay
 - LPNHE / Paris VI
- Germany
 - University of Bonn
 - HU Berlin
 - DESY
 - TU Dortmund
 - University of Göttingen
 - MPP & HLL Munich
- Italy
 - Università degli Studi di Udine -INFN
- Japan
 - KEK
- Spain
 - IFAE-CNM, Barcelona
- UK
 - University of Liverpool
 - University of Glasgow
- USA
 - UC Berkeley / LBNL
 - UNM, Albuquerque
 - UCSC, Santa Cruz

The probe station in the LAL clean room for IV and CV measurements:

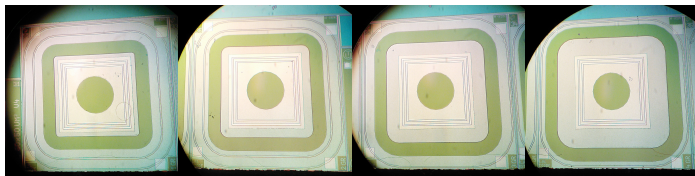


- Hardware set-up developed by N. Dinu, JF. Vagnucci, M. Benoit, A. Falou.
- IV and CV Labview programmes developed by M.Benoit.

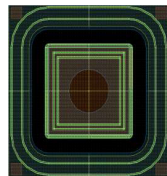
- Guard rings provide a controlled potential drop from the high voltage used for biasing the electrodes and the cutting edge of the device.
 - Usually this area is then inactive.
- Increasing the active area of pixel devices for future upgrades of ATLAS is important to minimise the material budget (and therefore reduce scattering before the calorimeters).
 - For the IBL the dead area was reduced from $\sim 1100 \mu\text{m} \rightarrow 200 \mu\text{m}$ by moving the edge pixels to partially underneath the guard rings.
 - LAL pixel group contributed to the IBL pixel design; ref: M. Benoit, PhD Thesis LAL 11-118 May 2011; N. Dinu, HDR LAL-13-192 October 2013
 - Diodes with different numbers of guard edge rings were included in the wafer production for 2011. New wafer production includes new diode designs.



- Guard rings provide a controlled potential drop from the high voltage used for biasing the electrodes and the cutting edge of the device.
 - Usually this area is then inactive.
- Increasing the active area of pixel devices for future upgrades of ATLAS is important to minimise the material budget (and therefore reduce scattering before the calorimeters).
 - For the IBL the dead area was reduced from $\sim 1100 \mu\text{m}$ \rightarrow $200 \mu\text{m}$ by moving the edge pixels to partially underneath the guard rings.
 - LAL pixel group contributed to the IBL pixel design; ref: M. Benoit, PhD Thesis LAL 11-118 May 2011; N. Dinu, HDR LAL-13-192 October 2013
 - Diodes with different numbers of guard rings were included in the wafer production for 2011. New wafer production includes new diode designs.

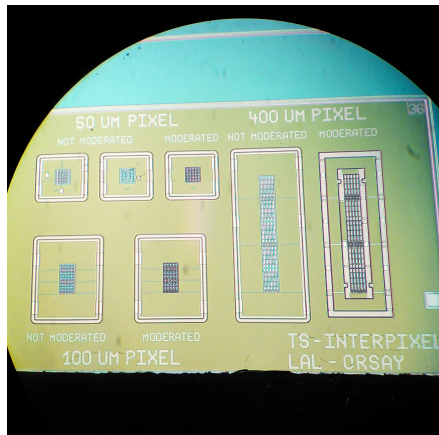


Diodes with varying numbers of guard rings. From 1-4.



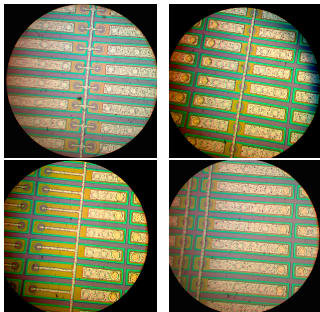
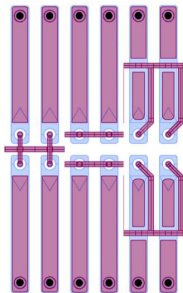
Preparation of new diode designs.

- Structures of various pixel size (50 μm , 100 μm and 400 μm).
 - Each structure contains a central pixel, 8 surrounding pixels (connected together) and 16 outer pixels (also connected together).
- Can study the inter-pixel capacitance of various designs.



Interpixel structure designed by N. Dinu

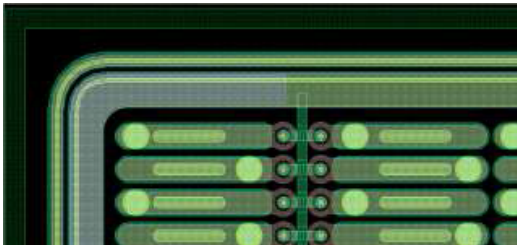
- FE-I4 compatible pixel sensors with alternative bias rail geometries to the current PPS layout.
- Aim is to find a solution that reduces the inefficiencies seen for this region within the pixel cell.
- Matrix contains several versions of bias rail geometry.



- All bias rail geometries photographed are on the same sensor, which is in the process of being flip-chipped and will be tested in the coming November test beam.

- The bias rail is metallisation on top of an insulator without an implant below. It provides a reference potential to each pixel and connects to virtual ground.

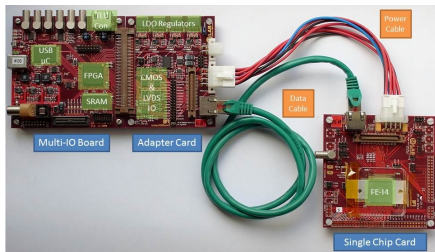
- Pixel size of $200 \times 35 \mu\text{m}$.
- Matrix of 24×96 pixels \rightarrow 5mm \times 5mm sensor size.
- Study of new, 3D read-out chips.
 - “an emerging, system level integration architecture wherein multiple strata (layers) of planar devices are stacked and interconnected using silicon (or other semiconductor material) vias (TSV) in the Z direction”¹
- New wafer production contains quad Omegapix modules.



[1]: Handbook of 3D Integration, edited by Philip Garrou, Christopher Bower and Peter Ramm.



- Setup of the USBPix test bench.
 - Test devices with the laser and strontium-90 source (a β -source) with external triggering.
 - Requires scintillators with photomultiplier tubes. These were obtained from CERN.

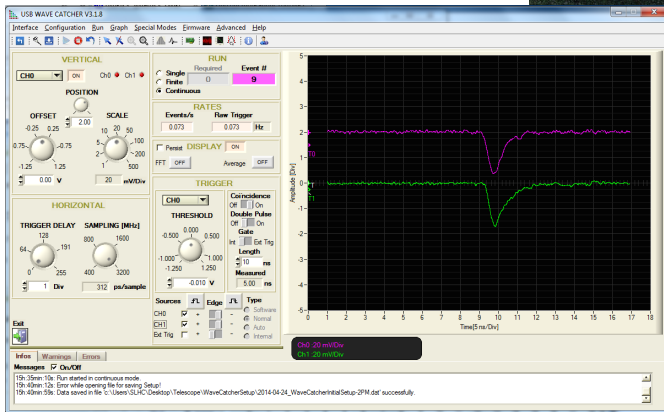
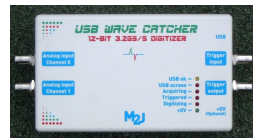


- USBPix is used to characterise the sensors.
 - Few hardware components, modular and portable.
- Data analysis using STcontrol software.



Trigger - wavecatcher

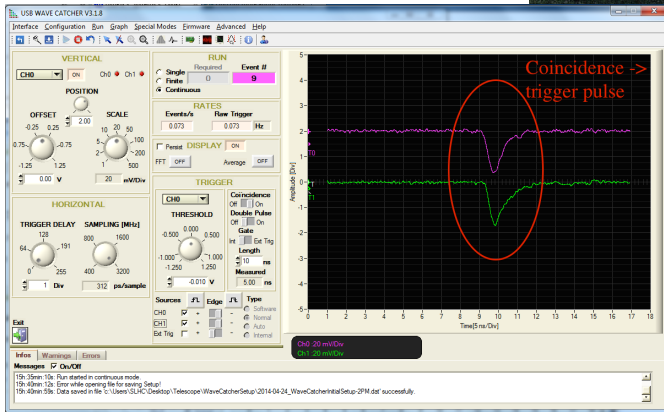
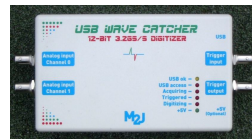
- Input is an analogue signal from the scintillators.
- Output as a digital trigger pulse from the coincidence of the two signals.



Ref: D. Breton, E. Delagnes, J. Maalmi, Using ultra fast analog memories for fast photodetector readout, NIMA, Volume 695, 11 Dec 2012, Pages 61-67, ISSN 0168-9002, <http://dx.doi.org/10.1016/j.nima.2011.12.007>.

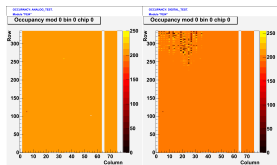
Trigger - wavecatcher

- Input is an analogue signal from the scintillators.
- Output as a digital trigger pulse from the coincidence of the two signals.

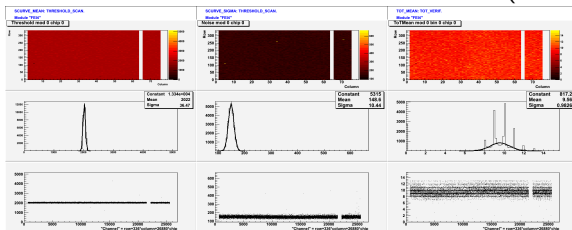


Ref: D. Breton, E. Delagnes, J. Maalmi, Using ultra fast analog memories for fast photodetector readout, NIMA, Volume 695, 11 Dec 2012, Pages 61-67, ISSN 0168-9002, <http://dx.doi.org/10.1016/j.nima.2011.12.007>.

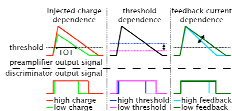
Analogue and digital:



Threshold, noise and Time Over Threshold (TOT):



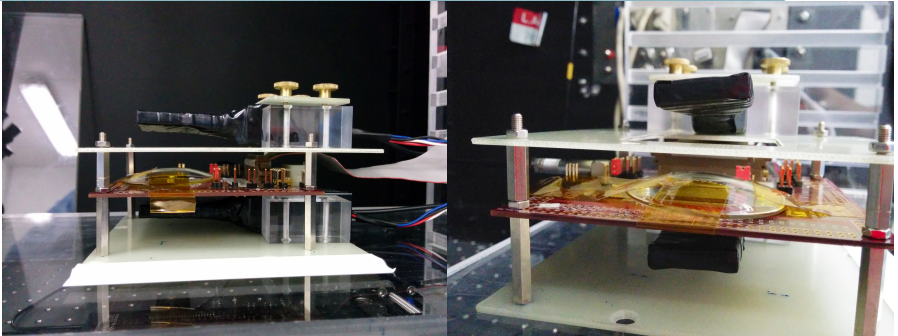
- The Analogue scan looks very good, but there is an issue in the top left of the Digital scan.
- This is understood and requires changing the Efuse_Cref parameter during the tuning.



How TOT and Threshold tuning effects the results.

TOT acceptable for proof-of-principle study.

Source scans - setup



- One scintillator above and one below.
- Top scintillator can be removed to place a source as close to the sensor as possible.
- Collimator plates are under production to focus the source beam to a small number of pixels.

Source scans

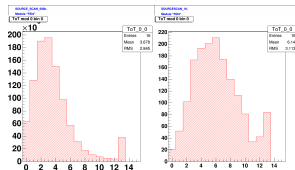
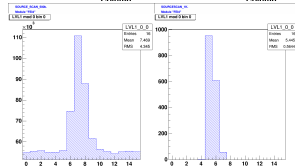
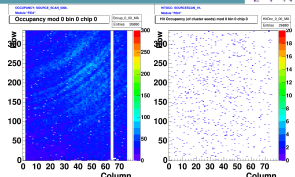
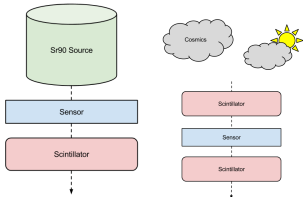
Performed source scans with various setups.
Initially at perpendicular angles:

1. Source scan with Strontium 90

- One scintillator
- 500k triggers

2. Source scan with cosmics

- Two scintillators
- 1k triggers



Hitmaps (top), Lvl1 distributions (middle) and TOT distributions (bottom) for strontium 90 scan (left) and cosmic scan (right).

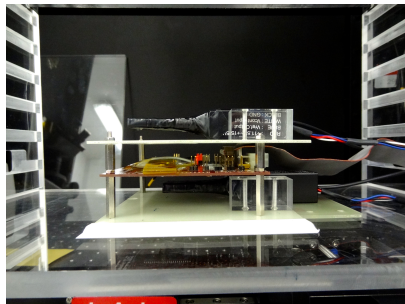
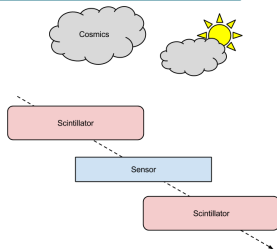
Proof of principle. Can we study cluster sizes by offsetting the scintillators?

1. Source scan with cosmics

- Two scintillators
- 500 triggers
- Each scintillator overlaps half of the sensor
- Data taking time = ~ 1 day

2. Source scan with cosmics

- Two scintillators
- 500 triggers
- Neither scintillator overlaps the sensor
- Data taking time = ~ 2 days



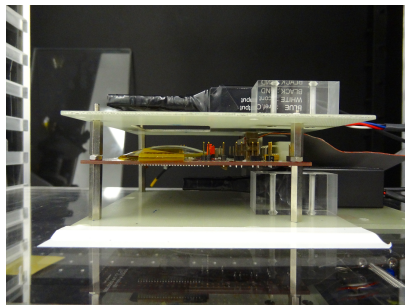
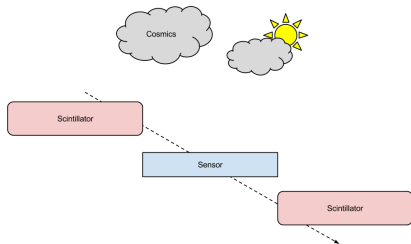
Proof of principle. Can we study cluster sizes by offsetting the scintillators?

1. Source scan with cosmics

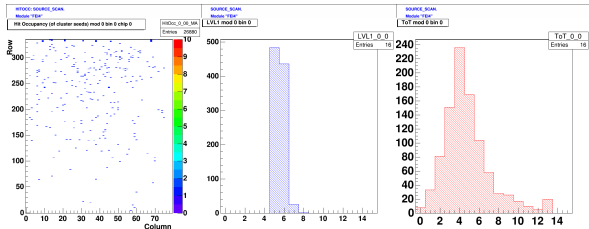
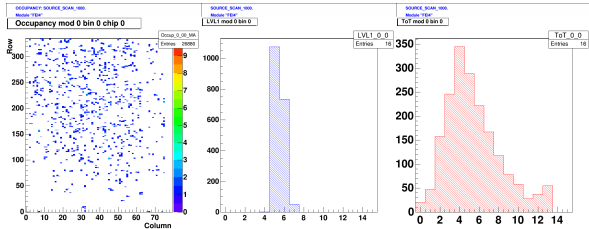
- Two scintillators
- 500 triggers
- Each scintillator overlaps half of the sensor
- Data taking time = ~ 1 day

2. Source scan with cosmics

- Two scintillators
- 500 triggers
- Neither scintillator overlaps the sensor
- Data taking time = ~ 2 days



Source scan results

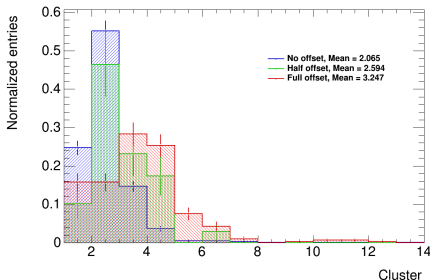


- Source scan with cosmics
 - Two scintillators
 - 500 triggers
 - Each scintillator overlaps half of the sensor

- Source scan with cosmics
 - Two scintillators
 - 500 triggers
 - Neither scintillator overlaps the sensor

Source scan results

Cluster Size as function of scintillator offset:



- Increase of cluster size as scintillator gap is increased (as expected).
 - Method can be used to study non-perpendicular tracks through the sensor when test beams are not available.
 - However, method is very slow and reconstruction of tracks is not available.
- With thanks to M. Bomben for sharing his adaption of C. Gallrapp's clustering programme.

Secondary Ion Mass Spectrometry (SIMS)



Interesting fact: The SIMS process will be used by ROSETTA to analyse the comet Churyumov-Gerasimenko (also known as 67P). DOI: 10.1002/rcm.2448. Image courtesy of ESA.

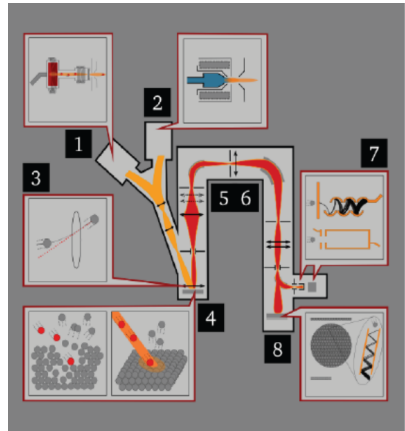


SIMS system at Versailles
(Cameca IMS 7F)

- For further information, please see: www.cameca.com;
Benninghoven et al. 1987

- Analytical technique to characterize the impurities in the surface and near surface ($\sim 30\mu\text{m}$) region
- Relies on sputtering of a primary energetic ion beam (0.5-20 keV) on sample surface and analysis of produced ionized secondary particles by mass spectrometry
- Good detection sensitivity for many elements such as: B, P, Al, As, Ni, O, Si etc.

- It can detect dopant densities as low as 10^{13} cm^{-3}
- Allows multi-element detection, has a **depth resolution of 1 to 5 nm** and can give a lateral surface characterization on a scale of several microns
- **Destructive method**, since the act of the removing material by sputtering leaves a crater in a sample
- It determines the **total dopant density profile**



- Dicing of 4" or 6" wafers which have been uniformly doped and not thinned.
- Measurements are taken after chemical oxide etching has been performed.
- Otherwise, for through-oxide measurements, no etching is performed.
- Sample preparation and measurements were done by:
 - Nicoleta Dinu
 - Sorin Dumitriu
 - Francois Jomard



Preparing the samples

n-in-n, CiS production, $\langle 100 \rangle$ orientation

Oxide thickness	100 nm							
P implantation doses	10^{13} cm^{-2}		10^{14} cm^{-2}		10^{15} cm^{-2}		10^{16} cm^{-2}	
Implantation energy (keV)	130	240	130	240	130	240	130	
Annealing	4 hours, 975 °C							

$\rho = 0.25 \Omega/\text{cm}$ ($3 \times 10^{16}/\text{cm}^3$), 380 μm thickness

n-in-p, ADVACAM production, $\langle 100 \rangle$ orientation, thickness $\leq 675 \mu\text{m}$

Oxide thickness	100 nm							
P implantation doses	10^{13} cm^{-2}		10^{14} cm^{-2}		10^{15} cm^{-2}		10^{16} cm^{-2}	
Implantation energy (keV)	130	240	130	240	130	240	130	240
Annealing	3 hours, 1000 °C							

$\rho = 0.2 - 0.25 \Omega/\text{cm}$ ($2.5 - 3 \times 10^{16}/\text{cm}^3$), 675 μm thickness

Further samples with 200nm oxide layer and high resistivity are available for SIM measurements, but will not be presented here.

Why Simulate?

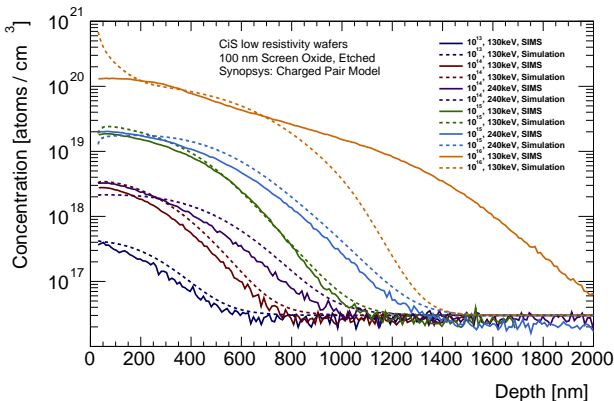


Sim City 1989 video game cover art. Image courtesy of Wikipedia.

- Results obtained from test structures can be used to develop reliable simulations of devices.
- Simulations, in turn, drive the development of new sensor layouts.
 - Quicker and less expensive than building multiple prototypes.
- Therefore, validation of simulation models is vital to trust predictions.
 - Studies of irradiated devices important for phase II upgrade.
- Simulation by Vagelis Gkougkousis

CiS Results

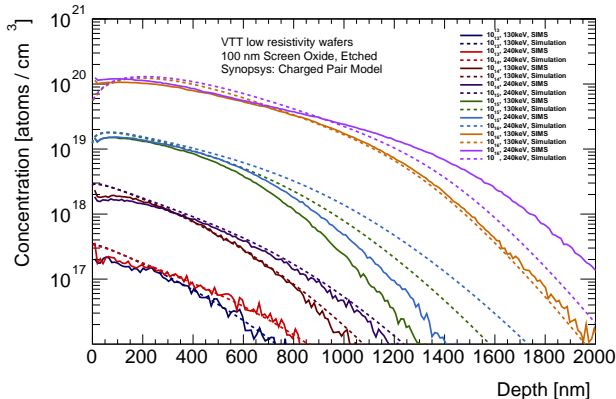
Simulation and data compared for CiS samples for Synopsys Charged Pair simulation model:



- Generally good agreement between simulation and SIMS data.
- Large discrepancy with the highest dose (10^{16}).

VTT Results

Simulation and data compared for VTT / ADVACAM samples for various Synopsys Charged Pair simulation model:



Reminder: VTT used a different annealing process to CiS.

The simulation process

Simulation is performed with Technology Computer Aided Design (TCAD). Two versions are considered here: Silvaco and Synopsys.

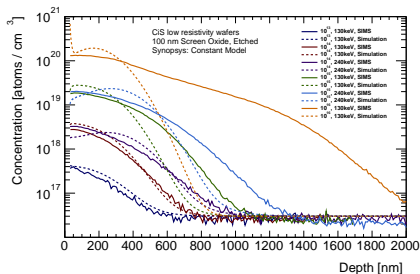
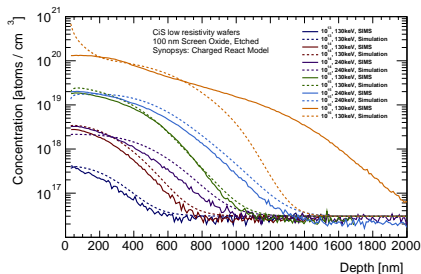
Silvaco

- Diffusion models:
 - **Fermi Model**
 - 4 CPL Model (clustering consideration)
 - PLS Solid State Model
- Oxidation process:
 - The parameters for oxidation are included in the simulation, rather than simply adding a layer of oxide on top.
- The simulation steps are taken from the manufacturer's own process flow.

Synopsys

- Programme used at LAL
- Diffusion models:
 - **Charged Pair Model**
 - Charged Fermi model
 - Constant Model
 - Charge React Model

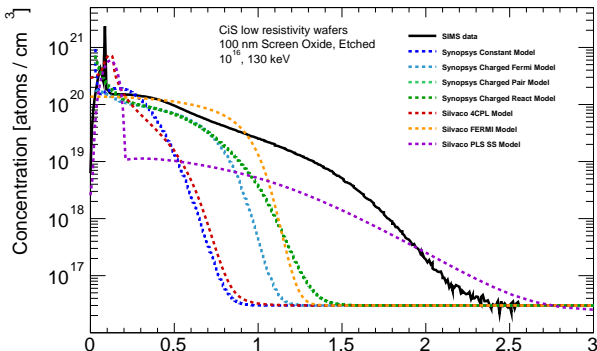
Simulations performed for **Charged React** (left) and **Constant** (right) models:



- Low and intermediate doses show relatively good agreement.
- For each model there is still a **discrepancy for the dose of 10^{16}** .
- Constant model shows the poorest comparison to data.

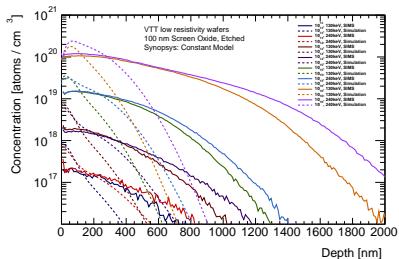
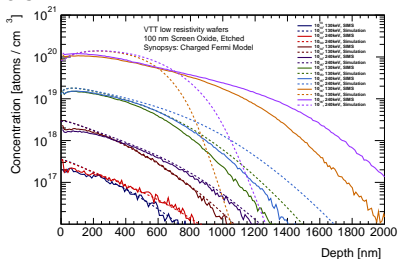
Comparison of models

Comparison of SIMS data and various simulation models from Synopsys and Silvaco for CiS sample with the **highest dose** (10^{16}).



No single model accurately simulates the SIMS data. Further work required, possibly to merge two models together (such as FERMI and PLS SS for Silvaco, combining the low dose and high dose simulation).

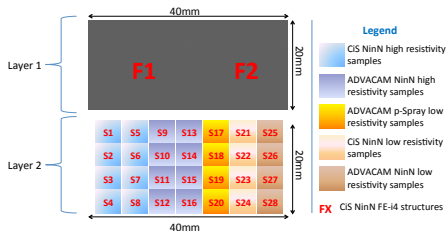
Simulations performed for **Charged Fermi** (left) and **Constant** (right) models:



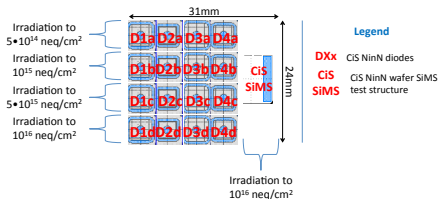
- Results for the Charged React model are not shown here due to the similarity with Charged Pair.
- Again, Constant model shows the poorest comparison to data.

Reminder: VTT used a **different annealing process** to **CiS**.

First group:

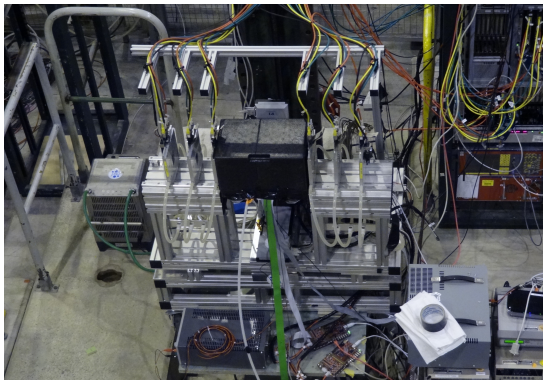


Second group:



- Irradiation plans for structures to be irradiated with protons at Karlsruhe, Germany.
- Intended fluence for irradiation for first layer is 10^{16} neq cm².
- Second layer, containing the SIMS structures, will be subject to a higher dose due to multiple scattering.
- Diodes will have varied irradiation levels to study this effect.
- Structures are bare \Rightarrow no UBMs.

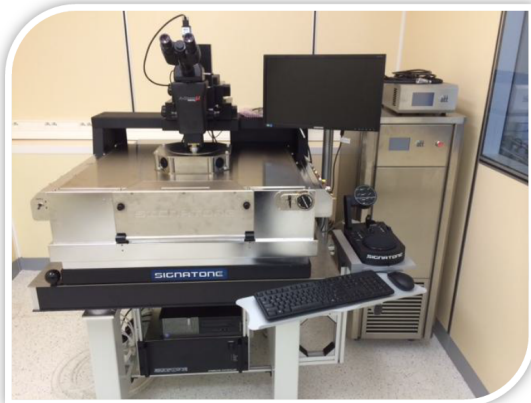
- Test beam measurements with CiS modules with alternative bias rail layouts coupled to ATLAS FE-I4 readout chip.
- Afterwards, irradiate modules to HL-LHC expected fluence levels ($\sim 1 \times 10^{-16}$) and re-test.



- Characterisation at LAL of novel pixel prototypes for the HL-LHC, including a method to study non-perpendicular tracks through an FE-I4 sensor, has been discussed.
 - Devices with alternative bias rail geometry are in preparation for test beam studies.
- Results have been presented for doping profile measurements performed with the SIMS method for samples from both CiS and VTT (ADVACAM). These measurements were compared with TCAD simulations for Synopsys and Silvaco.
 - Discrepancy observed between simulation and data for the highest doping profile for all simulation models for CiS structures.
 - Further studies for 200nm oxide layer and high resistivity wafers will be performed.
 - Samples will be irradiated to investigate what effect this will have on the active doping profile.

Final point

We like to share our toys:



New clean 100 m^2 room construction combined with acquisition of semi-automatic testing system machine (CAPTiNoV platform)

Thank you for your attention



Any questions?

Backup

•3D Simulation

Hypothetical fabrication process flow

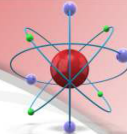
- Silicon Substrate
 - ❖ Type: p, Boron doped, $10^{14}/\text{cm}^3$
 - ❖ Orientation: 100, FZ type
 - ❖ Resistivity 100000 $\Omega\text{m}/\text{cm}^3$
 - ❖ Thickness: 150 μm (actual depth for simulation 5 μm)
 - ❖ O_2 content: $2.9 - 3.0 \cdot 10^{17}/\text{cm}^3$
- Oxide Layer
 - ❖ Bilateral thermal oxidation layer of 250nm (950 °C, 24h)
 - ❖ Bilateral Anisotropic etching
 - ❖ Second bilateral thermal oxidation layer of 70nm
- Photoresist
 - ❖ 1 μm isotropic deposition followed by strip etching after development
- n Implant (front side)
 - ❖ Phosphorus at 100keV, dose of 10^{15} particles/ cm^2 with angle of -90° through oxide layer

Concentration $10^{12} - 10^{13}$)

•3D Simulation

Hypothetical fabrication process flow

- p Implant (back side)
 - ❖ Boron at 40keV, dose of 10^{15} particles/cm² with angle of -90° through oxide layer
- Screen oxide etching and re-growing
 - ❖ Complete bilateral etch of the 70 nm damaged layer
 - ❖ Bilateral dry oxidation at 1050 °C, 150nm layer with subsequent implant drive in.
- Nitride layer
 - ❖ Bilateral Nitride LPCVD layer of 130 nm
 - ❖ Front side anisotropic etching for p-spray implantation
- Front side p-spray implant
 - ❖ Boron implantation at 120keV, 3.5×10^{12} particles/cm²



•3D Simulation

Hypothetical fabrication process flow

- Contacts etching and annealing
 - ❖ Annealing at 950C for 4h
 - ❖ Bilateral Oxide layer anisotropic etching to form metallization contacts
- Metallization deposition
 - ❖ LPCVD Aluminum bilateral deposition of 100nm layer
 - ❖ Front side anisotropic etching
 - ❖ Bilateral LTO (SiO_2) layer deposition of 300nm and etching to form passivation
- Edge passivation
 - ❖ 250 bilateral oxidation and etching
 - ❖ P-boron implantation at three angles (90, 45 & - 45 degrees) to form enveloping regions



From Sentaurus Process User Guide, Version E-2010.12, December 2010:

“During the fabrication process, dopants are introduced into the substrate with different concentration profiles. As processing proceeds through various thermal annealing cycles, the dopants diffuse and redistribute through the structure. The following effects contribute to dopant redistribution and can be modeled by Sentaurus Process:

- Dopant (de)activation
- Dopant-defect interaction
- Chemical reactions at interfaces and in bulk materials
- Material flow
- Moving material interfaces
- Internal electric fields”

From Sentaurus Process User Guide, Version E-2010.12, December 2010:

ChargedReact

"The React ... and ChargedReact ... diffusion models, also known as five-stream diffusion models, are the most advanced dopant diffusion models in Sentaurus Process. They solve up to three separate equations per dopant – a substitutional dopant – and up to two dopant-defect pairs and two defect equations. The ChargedReact model is the most accurate model available in Sentaurus Process. but because of the large number of equations required, it also is the most computationally expensive. The React model, which is an uncharged version of the ChargedReact model, is provided for backward compatibility."

ChargedPair

"The Pair ... and ChargedPair ... diffusion models, also known as three-stream diffusion models, assume that dopant-defect pairs are in local equilibrium but still solve for separate point-defect equations. These models solve one equation per dopant and two defect equations. The ChargedPair diffusion model allows the pairing coefficients to vary with charge state. These models are the most commonly used for advanced CMOS processes as they represent a balance between accuracy and computational expense. For extremely fast ramp rates or for customized initial conditions, the ChargedReact model or React model is a better choice. The Pair model, which is an uncharged version of the ChargedPair model, is provided for backward compatibility."

From Sentaurus Process User Guide, Version E-2010.12, December 2010:

ChargedFermi

"The Fermi ... and ChargedFermi ... diffusion models both assume that point defects as well as dopant-defect pairs are in equilibrium. The ChargedFermi diffusion model allows the diffusivity of each charge state to be set separately. An uncharged version of the model is provided for backward compatibility. These models can be used for longterm high-temperature anneals where the transient effect of annealing implant damage is minimal."

Constant

"The Constant diffusion model ..., unlike all other transport models, assumes a constant diffusivity and no electric-field effect, and is used mainly for dopant diffusion in oxide."